Communication

Circular Polarized Ground Radiation Antenna for Mobile Applications

Longyue Qu, Zeeshan Zahid, Hyung-Hoon Kim, and Hyeongdong Kim

***Abstract*— Here, we propose a ground radiation antenna (GradiAnt) with circular polarization (CP) by applying the ground-mode tuning (GMT) technique to the ground plane. We demonstrate that a GradiAnt at an arbitrary location of the ground plane can simultaneously excite two orthogonal modes of the same magnitude, and the phase difference between the two modes can be adjusted via GMT to achieve CP in mobile antennas. The proposed GradiAnt can be viewed as a combination of an electric coupler (J-type) and magnetic coupler (M-type) to the modes of the ground plane, and both modes can be excited to the same amplitude by tuning the coupling-type. GMT, applied to the ground modes using inductor-connected metal strips, can generate a 90° phase difference between the two modes of the ground plane. The proposed antenna design generates a 6 dB axial ratio bandwidth of 140 MHz from 2.38 to 2.52 GHz in the $+z$-direction. Right-hand CP and left-hand CP in the $+z$-direction and $-z$-direction, respectively, are obtained. The tuning mechanism is presented, and measurements are taken to validate the proposed technique.**

***Index Terms*— Circular polarization (CP), coupling-type, ground radiation antenna (GradiAnt), ground-mode tuning, mobile antennas.**

I. Introduction

Circular polarization (CP) reduces both polarization loss and multipath interference when compared with linear polarization, which is valued for its high-speed data transmission and reception [1], [2]. The conditions for CP require two orthogonal linear components in the same magnitude with a time-phase difference of 90° [2], [3]. CP has attracted considerable research attention [2]–[11], with most studies focusing on two methods of attaining CP: dual-orthogonal feeding [2]–[4] and single feeding [2], [3], [5]–[10]. Dual-orthogonal feeding suffers from complex implementation due to the need for a divider or hybrid. Single feeding is favorable for its simple implementation, and various antennas have been proposed, including microstrip [3], [5], [6], transformed dipole or monopole [7], [8], and slot or loop [9], [10]; however, both the generation of phase differences and the excitation of two orthogonal modes are difficult to achieve in mobile antennas. Normal mobile antennas can only achieve linear polarization [11]–[16] or dual polarization [17], and few studies have reported successful CP in mobile antennas. In [18], a ground radiation antenna (GradiAnt) is used to achieve CP by producing horizontal and vertical currents around the antenna structure; however, the ground effect is not included. In [19], the CP performance of the chip antenna is difficult to achieve in other platforms, and the antenna can only be located at the corner of the ground plane, restricting its applications.

In GradiAnts [15], [20]–[26] and ground-mode tuning (GMT) technique [25]–[28], it is important to note that small antennas dominantly radiate by exciting and utilizing the ground modes, and that a specific ground mode resonance can be tuned to match the target frequency. In this communication, CP is achieved by utilizing both GradiAnt and GMT, and we demonstrate that a single antenna at an arbitrary location of the ground plane can be used to simultaneously excite two orthogonal modes by tuning its coupling-type. The generation of CP using the proposed technique also confirms the functionality of a GradiAnt.

In this communication, a simple GradiAnt design is proposed for the implementation of CP for mobile applications. The coupling magnitude can be modified with each mode based on antenna-type, so that a GradiAnt at an arbitrary location can simultaneously excite the dominant modes along the x-axis and y-axis of the ground plane. To ensure a 90° phase difference between the two orthogonal modes, GMT is utilized and optimized by tuning the inductor value in the GMT structures. This communication is organized as follows. Section II presents the configuration of the proposed antenna design, Section III provides the simulation results and describes the tuning mechanism, and the proposed antenna is discussed in Section IV.

II. Antenna Design

Fig. 1 depicts the proposed antenna configuration, which is comprised GradiAnt and GMT structures. The structure of the GradiAnt is designed such that it can simultaneously excite the two dominant modes along the x-axis and y-axis of the ground plane (Mode 1 and Mode 2) to radiate. The GMT structures are designed to ensure that Mode 1 and Mode 2 are inductive and capacitive with a 90° phase difference at the operating frequency. Both antenna design and GMT can be optimized by observing the magnitude and the phase of the radiated fields, respectively. The proposed technique can be applicable to small-sized wireless devices, where the dominant modes along the length and width of the ground plane are normally higher than the operating frequency at 2.4 GHz, e.g., wearable devices or Internet of Things devices.

A ground plane with dimensions of 30 mm × 30 mm is etched in a 1 mm-thick FR4 substrate ($\varepsilon_r = 4.4$ and $\tan\delta = 0.02$). The proposed GradiAnt is located within a clearance of 3 mm × 15 mm at the upper side of the ground plane, fed by a capacitor CF (0.55 pF). At the left side of the GradiAnt, a 2.3 mm vertical section of the conductor line has a gap of 0.5 mm to the ground plane, producing distributed capacitance. Note that the width of all conductor lines is 0.5 mm. The proposed GradiAnt is located at the electric field maximum of Mode 1 and magnetic field maximum of Mode 2, so that a combination of electric coupler and magnetic coupler is desired. An electric coupler ($\boldsymbol{J}$-type) is coupled with the electric field of the ground plane as

$$\langle \text{antenna, mode} \rangle = \iiint \boldsymbol{J} \times \boldsymbol{E}\, d\tau$$

Manuscript received June 27, 2017; revised December 10, 2017; accepted February 26, 2018. Date of publication March 5, 2018; date of current version May 3, 2018. This work was supported by the ICT Research and Development Program of MSIP/IITP, South Korea, Ground Radiation Technique for Mobile Devices, under Grant 2013-0-00401. *(Corresponding author: Hyeongdong Kim.)*

L. Qu, Z. Zahid, and H. Kim are with the Department of Electronics Engineering, Hanyang University, Seoul 04763, South Korea (e-mail: rioinkorea@gmail.com; zeeshanzahid@mcs.edu.pk; hdkim@hanyang.ac.kr).

H.-H. Kim is with the Department of Biomedical Engineering, Kwangju Women's University, Gwangju 506713, South Korea (e-mail: hhkim@kwu.ac.kr).

Color versions of one or more of the figures in this communication are available online at http://ieeexplore.ieee.org.

Digital Object Identifier 10.1109/TAP.2018.2811840

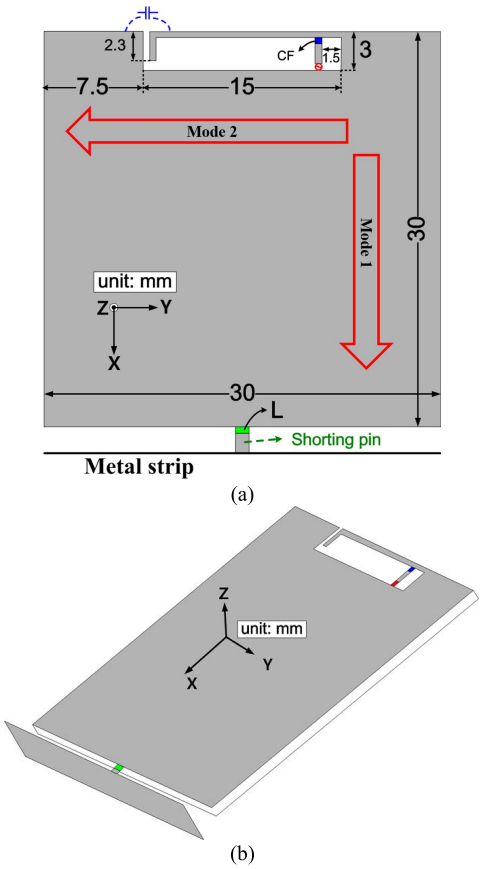

Fig. 1. Configuration of the proposed antenna. (a) Front view. (b) 3-D view.

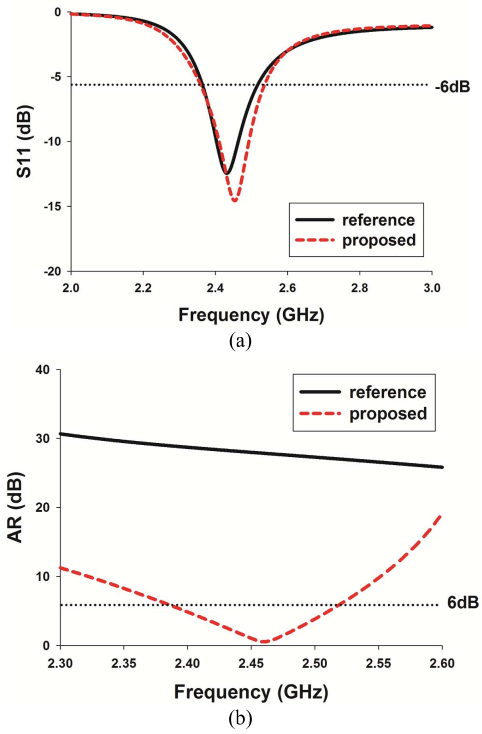

Fig. 2. (a) Simulated input impedance in a Smith chart. (b) AR values.

and a magnetic coupler ($\boldsymbol{M}$-type) is coupled with the magnetic fields of the ground plane as

$$\langle \text{antenna, mode} \rangle = -\iiint \boldsymbol{M} \times \boldsymbol{H}\, d\tau$$

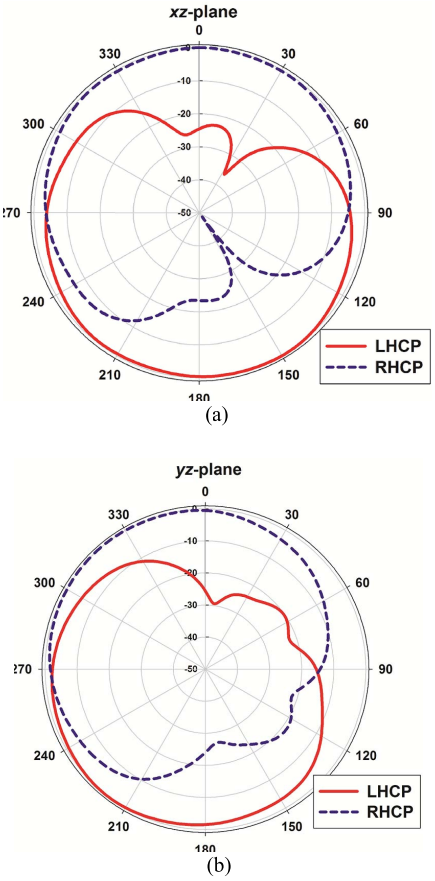

Fig. 3. Normalized radiation pattern at 2.45 GHz in the (a) xz plane and (b) yz plane.

where $\boldsymbol{J}$ and $\boldsymbol{M}$ are the coupling-types of the antenna, and $\boldsymbol{E}$ and $\boldsymbol{H}$ are the electric and magnetic fields of the ground mode. Therefore, a $\boldsymbol{J}$-type can capacitively couple with Mode 1, while an $\boldsymbol{M}$-type can inductively couple with Mode 2 [13], [25]. Accordingly, we can use a single antenna at an arbitrary location to simultaneously excite and utilize Modes 1 and 2 for radiation, which forms the basic principle of the proposed technique.

For the small ground plane without GMT, the resonant frequencies of both dominant modes are higher than the operating frequency. To satisfy the conditions of CP, GMT is adopted to generate a phase difference between Modes 1 and 2. The GMT structures are proposed in the bottom of the ground plane, which comprises a metal strip and a shorting pin. The metal strip is located 2 mm away from the ground plane, with a length of 30 mm, and height of 4 mm along the z-axis. The shorting pin is used for connection at the midpoint of the bottom of the ground plane through an inductor L (1.7 nH), so that the resonant frequency of Mode 1 can be tuned easily. To maintain polarization purity, a specific ground mode should be controlled without affecting another, so the shorting pin is preferred to be implemented near the center of the edge of the ground plane. The GMT effect is determined by both the metal strip and the loaded inductor, which can provide shunt capacitance and inductance to the ground mode, as discussed in [25] using an equivalent circuit model and its input admittance equation. Note that a planar closed loop can also be utilized as another possible GMT structure candidate [29]. Mode 2 can also be tuned if necessary. The phase difference between Modes 1 and 2 is the most difficult condition to attain in mobile devices, as well as GMT. The antenna design without GMT is designated the reference design for the sake of comparison.

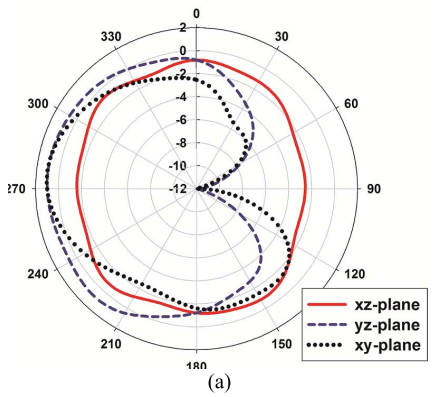

(a)

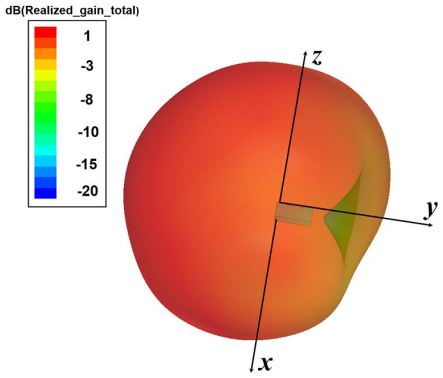

(b)

Fig. 4. Simulated total radiation patterns in realized gain at 2.45 GHz. (a) Radiation patterns in the *xz*, *yz*, and *xy* planes. (b) 3-D radiation pattern.

III. Simulation Results and Tuning Mechanism

A. Simulation Results

Fig. 2(a) presents the simulated reflection coefficients of the reference and proposed designs. The 3:1 VSWR bandwidth of the proposed design is 170 MHz from 2.36 to 2.53 GHz, fully covering the operating frequency band for WLAN applications. The impedance bandwidth of the reference design is from 2.36 to 2.51 GHz, which is similar to that in the proposed design.

The axial ratio (AR) is an important parameter in characterizing the polarization performance, which ranges from 0 dB to infinity. The AR curves of the reference and proposed antenna designs are obtained in the $+z$-direction, as shown in Fig. 2(b). The 6 dB AR bandwidth of the proposed antenna design is 140 MHz, ranging from 2.38 to 2.52 GHz, indicating that CP is generated by simultaneously exciting both Modes 1 and 2 of the ground plane. The AR values in the reference design are notably high, because the two modes of the ground plane cannot satisfy the phase difference. Therefore, the proposed antenna design can provide CP without greatly affecting impedance bandwidth performance.

The simulated radiation patterns of the proposed antenna at 2.45 GHz are presented in Fig. 3 for a comprehensive view of the polarization performance. In the *xz* plane, the antenna generates right-hand circular polarization (RHCP) in the $+z$-direction and left-hand circular polarization (LHCP) in the $-z$-direction, as shown in Fig. 3(a). RHCP and LHCP are also generated in the $+z$-direction and $-z$-direction, respectively, in the *yz* plane [Fig. 3(b)]. The total radiation patterns of the proposed antenna are presented to evaluate its radiation performance (Fig. 4). From the *xz*, *yz*, and *xy* planes in Fig. 4(a), it can be observed that the proposed antenna produces radiation patterns with a minimum realized gain of -12 dBi in the null direction, indicating that the antenna is less directional.

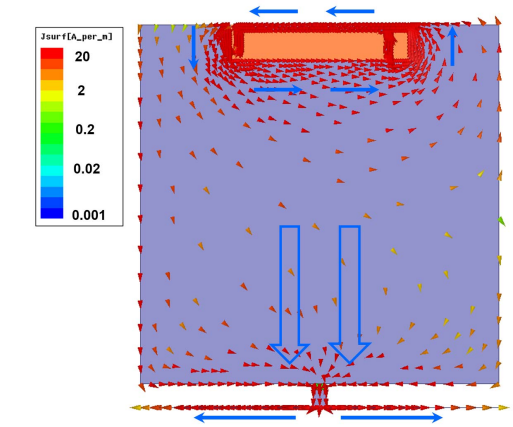

(a)

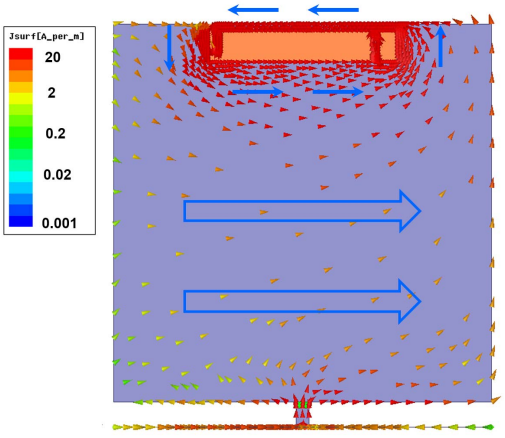

(b)

Fig. 5. Simulated surface-current distributions at 2.45 GHz at a phase of (a) 0° and (b) 90°.

Furthermore, the 3-D radiation pattern is also shown in Fig. 4(b), and the radiation null is generated along the *y*-axis. Though the radiation pattern is not isotropic, the difference between the peak gain (1 dBi) and the null gain (-12 dBi) is significantly reduced compared to the linearly polarized antenna, which is a favorable characteristic in transmission and reception.

To further validate the polarization performance of the proposed antenna, the simulated current distributions are shown at 2.45 GHz in Fig. 5. As shown in Fig. 5(a), the current distributions over the ground plane are directed along the *x*-axis at a phase of 0°. The current flows into the GMT structures, so that Mode 1 is operating. At a phase of 90° [Fig. 5(b)], the current distributions over the ground plane are directed in the *y*-axis, so that Mode 2 is operating. Both the feeding location and the time-phase difference of the two orthogonal modes in the ground plane determine the generation of RHCP in the $+z$-direction and LHCP in the $-z$-direction. It is important to observe that the total current distribution around the antenna area cancel with each other, operating as a transmission-line (nonradiating) mode, which contribute only to the excitation of the ground modes [15], [20]–[26].

B. Tuning Mechanism

The proposed GradiAnt plays an important role in exciting the two orthogonal and perpendicular modes of the ground plane, and the coupling between the antenna and the ground modes is dependent on its coupling-type and location in the ground plane, which are evaluated and investigated as follows.

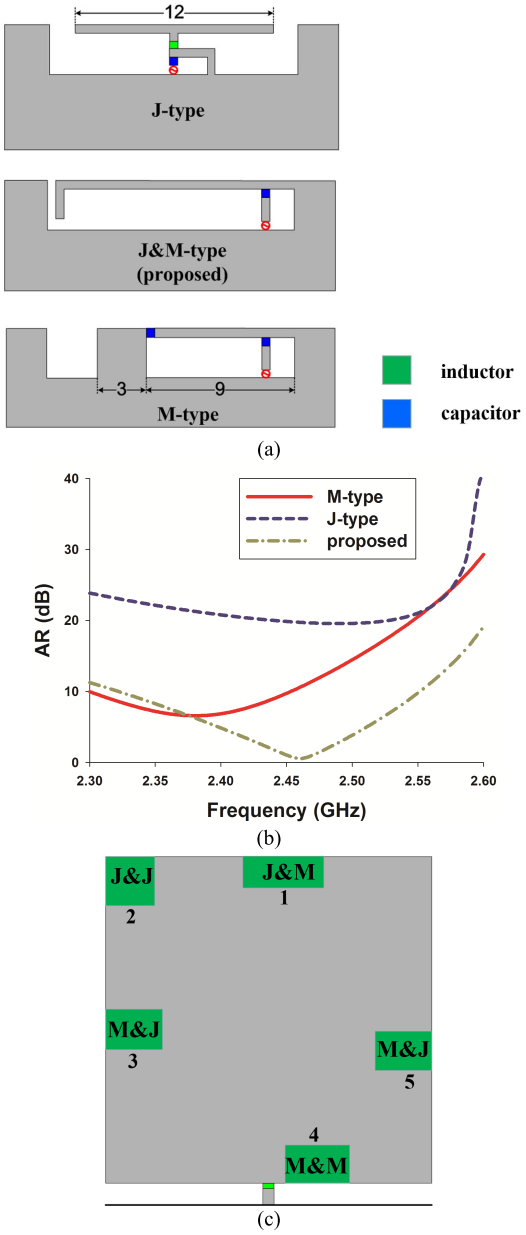

Fig. 6. Antenna coupling-type-based AR variation. (a) Antenna types. (b) AR variation. (c) Coupling-type and antenna location.

Three different antenna coupling types were implemented and are shown in Fig. 6(a); their polarization properties are shown in Fig. 6(b). In Fig. 6(a), the ***J***-type antenna operates by coupling with the electric field of Mode 1 [13], [30], and the ***M***-type antenna operates by coupling with the magnetic fields of Mode 2 [25], [30]. Fig. 6(b) presents simulated AR curves in the $+z$-direction that were generated using various coupling types of GradiAnt. As shown, ***J***-type or ***M***-type GradiAnts result in higher values of AR, because either type can dominantly excite only Mode 1 or Mode 2. Therefore, we propose a combination ***J&M***-type that can simultaneously excite both ground modes, obtaining good CP performance.

Though the proposed antenna has been chosen in Location 1 as a case study, further investigation of the coupling-type and antenna location is discussed in Fig. 6(c). When the antenna location shifts from Location 1 to Location 2, the magnetic field of Mode 2 decreases and the electric field increases, so that a more electrically coupled antenna-type for Mode 2 should be designed, and vice versa.

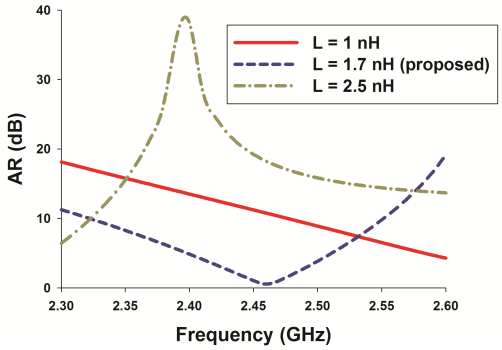

Fig. 7. AR variation by tuning the value of L in the GMT structures.

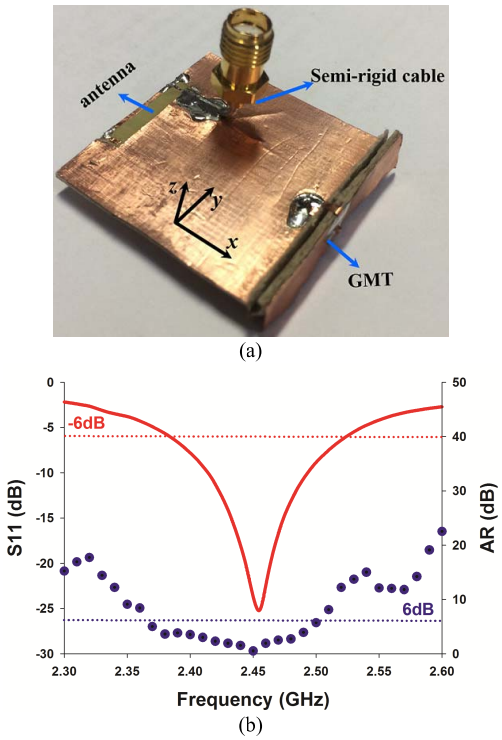

Fig. 8. Measured results of the fabricated antenna design. (a) Fabrication of the proposed antenna. (b) Measured S_{11} and AR curve.

Accordingly, the ***J&M***-type antenna is progressively transformed into a ***J&J***-type one, which is the case in [19]. Therefore, a corresponding coupling-type that is suitable for simultaneous coupling to both modes can be developed at an arbitrary location. For example, an ***M&J***-type antenna is necessary in Locations 3 and 5 to excite Modes 1 and 2, while an ***M&M***-type one is preferred in Location 4.

Another critical factor to CP generation is the GMT structures. As is stated, phase difference between Mode 1 and Mode 2 can be generated only by GMT without changing the dimensions of the ground plane. Therefore, the effect of GMT is verified by tuning the values of L, which is shown in Fig. 7. By increasing the value of L, the resonant frequency of Mode 1 is lowered down, further affecting the phase difference. Either increasing or decreasing the value of L will lead to higher AR. Therefore, GMT is another important tuning parameter.

IV. Measurement Results

To verify the proposed technique, the antenna design is fabricated and measured in a 3-D CTIA OTA chamber, as shown in Fig. 8(a). The measured reflection coefficient is presented in Fig. 8(b), and the

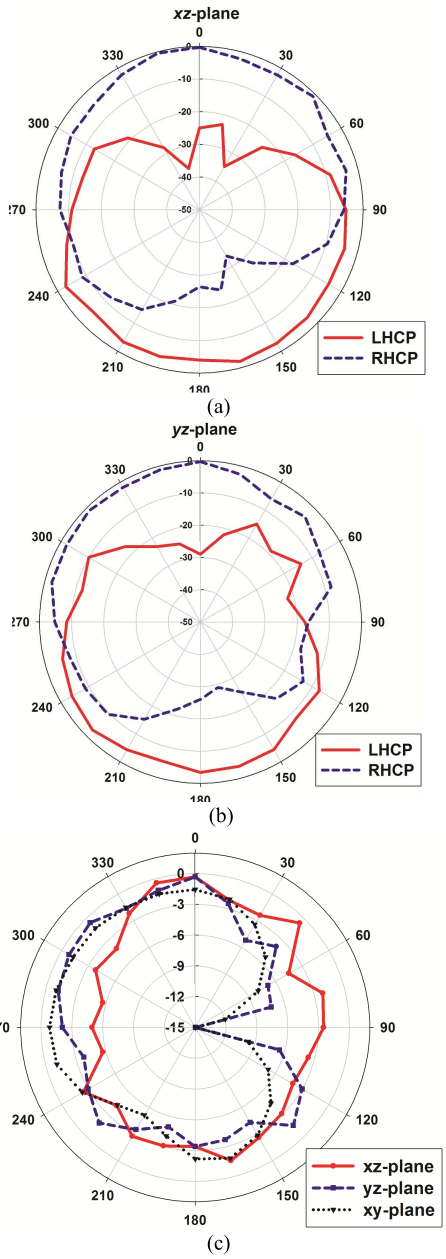

Fig. 9. Measured radiation patterns of the proposed antenna at 2.45 GHz. (a) *xz* plane. (b) *yz* plane. (c) Total radiation patterns in the *xz*, *yz*, and *xy* planes.

3:1 VSWR bandwidth is from 2.38 to 2.52 GHz, which is consistent with the simulation results. Furthermore, the AR curve is shown in Fig. 8(b), where the 6 dB AR bandwidth is from 2.36 to 2.50 GHz, which agrees well with the simulation. The measured polarization patterns in the *xz* and *yz* planes are shown in Fig. 9(a) and (b), and it can be observed that RHCP and LHCP are generated in the $+z$-direction and $-z$-direction, respectively. The total radiation patterns in *xz*, *yz*, and *xy* planes are demonstrated in Fig. 9(c), where a minimum gain of -15 dBi and a maximum gain of 0.77 dBi are produced by the proposed antenna. Therefore, the measurement results are in agreement with the simulation results, and the slight difference can mainly be attributed to the induced current flow onto the semirigid cable.

V. Conclusion

A GradiAnt with CP is proposed for mobile applications. The proposed GradiAnt can be tuned to various coupling types to simultaneously excite two orthogonal modes of the ground plane with the same magnitude. GMT is applied to the ground plane, so that the desired phase difference between the two modes is generated. The proposed GradiAnt can generate a 3:1 VSWR bandwidth of 170 MHz and a 6 dB AR bandwidth of 140 MHz in a small ground plane. RHCP and LHCP are generated in the $+z$-direction and $-z$-direction, respectively. The proposed technique confirms an important fact: that a mobile antenna is a GradiAnt that excites and utilizes ground modes for radiation.

References

[1] R. G. Vaughan, "Polarization diversity in mobile communications," *IEEE Trans. Veh. Technol.*, vol. 39, no. 3, pp. 177–186, Aug. 1990.

[2] C. A. Balanis, *Antenna Theory: Analysis and Design*, 4th ed. Hoboken, NJ, USA: Wiley, 2016.

[3] R. Garg, P. Bhartia, I. Bahl, and A. Ittipiboon, *Microstrip Antenna Design Handbook*. Norwood, MA, USA: Artech House, 2001.

[4] W. Lin and H. Wong, "Wideband circular polarization reconfigurable antenna," *IEEE Trans. Antenna Propag.*, vol. 63, no. 12, pp. 5938–5944, Dec. 2015.

[5] K. L. Chung and A. S. Mohan, "A systematic design method to obtain broadband characteristics for singly-fed electromagnetically coupled patch antennas for circular polarization," *IEEE Trans. Antennas Propag.*, vol. 51, no. 12, pp. 3239–3248, Dec. 2003.

[6] K. M. Mak, H. W. Lai, K. M. Luk, and K. L. Ho, "Polarization reconfigurable circular patch antenna with a C-shaped," *IEEE Trans. Antennas Propag.*, vol. 65, no. 3, pp. 1388–1392, Mar. 2017.

[7] C. Morlaas, B. Souny, and A. Chabory, "Helical-ring antenna for hemispherical radiation in circular polarization," *IEEE Trans. Antennas Propag.*, vol. 63, no. 11, pp. 4693–4701, Nov. 2015.

[8] T. Fujimoto and K. Jono, "Wideband rectangular printed monopole antenna for circular polarisation," *IET Microw. Antennas Propag.*, vol. 8, no. 9, pp. 649–656, 2014.

[9] C.-J. Wang and W.-B. Tsai, "Microstrip open-slot antenna with broadband circular polarization and impedance bandwidth," *IEEE Trans. Antennas Propag.*, vol. 64, no. 9, pp. 4095–4098, Sep. 2016.

[10] S. A. Rezaeieh, A. Abbosh, and M. A. Antoniades, "Broadband planar circularly polarised antenna for ultra-high frequency applications," *IET Microw., Antennas Propag.*, vol. 8, no. 4, pp. 263–271, Mar. 2014.

[11] Z. Zhang, *Antenna Design for Mobile Devices*. Hoboken, NJ, USA: Wiley, 2011.

[12] K.-L. Wong and Y.-C. Chen, "Small-size hybrid loop/open-slot antenna for the LTE smartphone," *IEEE Trans. Antennas Propag.*, vol. 63, no. 12, pp. 5837–5841, Dec. 2015.

[13] P. Vainikainen, J. Ollikainen, O. Kivekas, and I. Kelander, "Resonator-based analysis of the combination of mobile handset antenna and chassis," *IEEE Trans. Antennas Propag.*, vol. 50, no. 10, pp. 1433–1444, Oct. 2002.

[14] L. Qu, H. Lee, H. Shin, M.-G. Kim, and H. Kim, "MIMO antennas using controlled orthogonal characteristic modes by metal rims," *IET Microw., Antennas Propag.*, vol. 11, no. 7, pp. 1009–1015, Feb. 2017.

[15] L. Qu, R. Zhang, H. Kim, and H. Kim, "Compact dual-band antenna using inverted-L loop and inner rectangular loop for WLAN applications," *Electron. Lett.*, vol. 51, no. 23, pp. 1843–1844, 2015.

[16] K.-L. Wong and C.-Y. Tsai, "Small-size stacked inverted-F antenna with two hybrid shorting strips for the LTE/WWAN tablet device," *IEEE Trans. Antennas Propag.*, vol. 62, no. 8, pp. 3962–3969, Aug. 2014.

[17] X. Zhao, B. N. Tian, S. P. Yeo, and L. C. Ong, "Wideband segmented loop antenna with dual-polarized omnidirectional patterns for mobile platforms," *IEEE Trans. Antennas Propag.*, vol. 65, no. 2, pp. 883–886, Feb. 2017.

[18] W. Lei, H. Chu, and Y.-X. Guo, "Design of a circularly polarized ground radiation antenna for biomedical applications," *IEEE Trans. Antennas Propag.*, vol. 64, no. 6, pp. 2535–2540, Jun. 2016.

[19] W.-J. Liao, J.-T. Yeh, and S.-H. Chang, "Circularly polarized chip antenna design for GPS reception on handsets," *IEEE Trans. Antennas Propag.*, vol. 62, no. 7, pp. 3482–3489, Jul. 2014.

[20] L. Qu, R. Zhang, and H. Kim, "High-sensitivity ground radiation antenna system using an adjacent slot for Bluetooth headsets," *IEEE Trans. Antennas Propag.*, vol. 63, no. 12, pp. 5903–5907, Dec. 2015.

[21] L. Qu, R. Zhang, H. Lee, and H. Kim, "Compact triple-band ground radiation antenna using two inner rectangular loops enclosed by two outer loops," *Electron. Lett.*, vol. 52, no. 10, pp. 790–792, May 2016.

[22] L. Qu, R. Zhang, and H. Kim, "Decoupling between ground radiation antennas with ground-coupled loop-type isolator for WLAN applications," *IET Microw., Antennas Propag.*, vol. 10, no. 5, pp. 546–552, 2016.

[23] H. Choi, J. Lee, O. Cho, X. Lu, and J.-H. Jang, "Ground radiation antenna," U.S. Patent 8 581 799 B2, Nov. 12, 2011.

[24] Y. Liu, H.-H. Kim, and H. Kim, "Loop-type ground radiation antenna for dual-band WLAN applications," *IEEE Trans. Antennas Propag.*, vol. 61, no. 9, pp. 4819–4823, Sep. 2013.

[25] L. Qu, R. Zhang, H. Shin, J. Kim, and H. Kim, "Mode-controlled wideband slot-fed ground radiation antenna utilizing metal loads for mobile applications," *IEEE Trans. Antennas Propag.*, vol. 65, no. 2, pp. 867–872, Feb. 2017.

[26] L. Qu, R. Zhang, H. Shin, J. Kim, and H. Kim, "Performance enhancement of ground radiation antenna for Z-wave applications using tunable metal loads," *Electron. Lett.*, vol. 52, pp. 1827–1828, Oct. 2016.

[27] C.-H. Chang and K.-L. Wong, "Bandwidth enhancement of internal WWAN antenna using an inductively coupled plate in the small-size mobile phone," *Microw. Opt. Technol. Lett.*, vol. 52, no. 6, pp. 1247–1253, Jun. 2010.

[28] W. L. Schroeder, C. T. Famdie, and K. Solbach, "Utilisation and tuning of the chassis modes of a handheld terminal for the design," in *Proc. IEE Wideband Multi-Band Antennas Arrays*, Birmingham, U.K., Sep. 2005, pp. 117–121.

[29] S. Yo, L. Qu, J. Kim, and H. Kim, "Mobile antenna performance improvement by ground mode tuning using a closed loop," *IET Microw. Antennas Propag.*, vol. 11, no. 8, pp. 1121–1126, Jun. 2017.

[30] R. F. Harrington, *Time-Harmonic Electromagnetic Fields*. New York, NY, USA: McGraw-Hill, 1961.